A STUDY OF THE REACTION $\pi p \to \Delta\rho$ AT 50 GeV/c

R. A. Carrigan,Jr. and A. W. Key
National Accelerator Laboratory

E. C. Fowler
Brookhaven National Laboratory and Duke University

and

J. D. Prentice
University of Toronto

ABSTRACT

An experiment has been designed to investigate the reaction $\pi^{\pm}p \to \rho^{o}\Delta^{++}$ at a beam momentum of 50 GeV/c. The apparatus consists of a 4π detector surrounding the target region and a large downstream spectrometer with two magnets and interspersed wire planes. Both wire planes and a rapid-cycling bubble chamber are considered for the target region. For full acceptance of the downstream rho meson, the first magnet, with a field of 20 kG, has a field volume 2 m long, 2.32 m wide, and 0.86 m high; the second magnet, with a field of 40 kG, is 4 m long, 2.4 m wide, and 1.45 m high. The resulting apparatus has sufficient mass resolution to identify the unstable particle masses and give good $|t|$ resolution.

I. INTRODUCTION

This report describes the design of an experiment to study the reaction $\pi^{\pm}p \to \rho^{o}\Delta^{++} \to \pi^{+}\pi^{-}p\pi^{\pm}$. We have chosen this specific reaction for two reasons: (1) It is of considerable theoretical interest. (2) It is an example of a class of reactions in which a quasi two-body final state is peripherally produced and both particles subsequently decay. By considering a fairly detailed design for this specific reaction, we believe we have identified the problems involved in generalizing the apparatus to a large class of reactions of this type.

It has been pointed out that this reaction gives a crucial test of the suggestion that a second Regge trajectory conspires with the pion to give the sharp forward peak in $np \to pn$ charge exchange scattering. LeBellac[1] has shown that conspiracy predicts a dip as $t \to 0$ in the ρ_{00} element of the ρ density matrix. The only experimental

check of this prediction which has been published[2] concludes that this dip is not observed. However, owing to the rather low bombarding energy of this experiment (8 GeV/c $\pi^+ p \to \rho^o \Delta^{++}$) the minimum value of t observable is rather high and is strongly dependent on the masses of the ρ and Δ both of which have a considerable mass width. The absence of the dip can thus only be demonstrated at this bombarding energy by plotting $d\sigma/dt$ vs t', where $t' = t - t_{min}$ calculated with the t_{min} appropriate to the particular masses of each event. This procedure has been justified by Donohue[3] but it is clearly of interest to check these conclusions at higher bombarding energies. The variation of the cross section with s over a large range will also check the validity of the assumption that this reaction can be described in terms of the exchange of the pion Regge trajectory.

This experiment, as mentioned above, is an example of a class in which two unstable particles are produced with low momentum transfer, and in which it is important to measure the decay angular distributions of both of them. To achieve this with good efficiency and without angular bias, it is necessary to detect the decay products of the nucleon resonance with as near to 4π solid angle as possible and to measure the angles and momenta of the fast forward particles with high accuracy.

II. GENERAL FEATURES OF THE REACTION $\pi^{\pm} p \to \rho^o \Delta^{o,++}$

Beam and Cross Section

The apparatus described below is equally applicable to the two reactions $\pi^+ p \to \rho^o \Delta^{++}$ (1) and $\pi^- p \to \rho^o \Delta^o$ (2). Each has certain advantages. Assuming a one pion exchange production mechanism, the rate for the final state $\pi^+\pi^-p\pi^+$ from reaction (1) is expected to be 9 times the rate for the $\pi^+\pi^-p\pi^-$ final state from reaction (2). This ratio is due to the I-spin Clebsch-Gordan coefficients for the production and decay processes. This advantage for the positive beam must be weighed against the contamination of 27% protons and 2.8% K^+ which is present in the positive beam. The negative beam is almost pure π^- (97%), with only 1.8% K^- and 1.2% $\bar{p}$. (These numbers have been supplied by the Beam Group at this Summer Study.) The higher contamination would lead to a higher proportion of unwanted triggers in the π^+ experiment and would require considerable added computing of kinematic fits to reject the proton-induced events. An alternative solution is to make use of beam tagging with the DISCS which have been recommended for one branch of the 2.5 mrad beam. This would open up the possibility of simultaneously studying the reactions

$$pp \to \Delta^o \Delta^{++}$$

$$K^+ p \to K^{*o}(890)\Delta^{++}$$
$$\qquad\quad \hookrightarrow K^+\pi^-$$

in the positive beam case and the reactions

$$K^-p \to K^{*o}\Delta^o$$
$$\quad\quad \hookrightarrow K^-\pi^+$$
$$\to \rho^o\Lambda^o$$
$$\bar{p}p \to \overline{\Delta^{++}}\Delta^{++}$$

with the negative beam. We have, therefore, included some kinematics for these cases (Appendix B).

We have selected a beam momentum of 50 GeV/c. This is above the range that is likely to be covered before 1972 but is sufficiently low that we can expect a reasonable cross section to remain for reaction (1). The cross section is $430 \pm 40\,\mu b$[4] at 8 GeV/c (s = 16). Using the figures of Strauch[5] in the 1968 Summer Study for the 20 GeV/c cross sections for $\pi^-p \to \pi^-\pi^+p\pi^-$ (890 μb), $\pi^-p \to \rho^o p\pi^-$ (540 μb), $\pi^-p \to A_2^-p$ (160 μb) and $\pi^-p \to \pi^+\pi^-N^{*o}$ (52 μb) we estimate

$A_2^- \hookrightarrow \rho^o\pi^-$ $\quad\quad N^{*o} \hookrightarrow \pi^-p$

$\sigma(\pi^-p \to \rho^o N^{*o}) = (540 - 160)/890 \times 52\ \mu b = 22 \pm 4\ \mu b$. This cross section is for s = 38. This implies a cross section for reaction (1) of 198 ± 36 μb. This in turn implies a variation of $\sigma(\pi^+p \to \rho^o\Delta^{++})$ as s^{-1}. Extrapolating to 50 GeV/c (s = 95), we estimate a cross section of 86 ± 40 μb for reaction (1) and thus 9.5 ± 4.5 μb for reaction (2). As the Regge trajectory of the pion passes very close to the origin $s^{2\alpha - 2} \approx s^{-2}$ for small t. It is perhaps safer then to assume that the cross section for 50 GeV/c lies at the lower limit of the error ranges quoted, i.e. 46 μb for reaction (1) and 5 μb for reaction (2). Figure 1 shows the cross-section behavior as a function of s for $\pi^+p \to \rho^o\Delta^{++}$. A fit[4] of the functional form e^{At} to the plot of $d\sigma/dt$ vs t for reaction (1) at 8 GeV/c gives for $0 < -t < 0.4\ GeV^2$, a value of $A = 11.7 \pm 1.1\ GeV^{-2}$. We therefore expect the reaction to be highly peripheral at 50 GeV/c.

Kinematic Calculations

To determine the design requirements for the downstream spectrometer and target detector system, a two-body kinematics program written by L. Leipuner was modified to calculate the production angles and momenta of two resonances of arbitrary mass and the subsequent decay of each into two particles. For simplicity the calculations were done for the case in which all four final-state particles are coplanar. This defines the maximum and minimum angles and momenta necessary for aperture calculations. The results of these calculations are discussed in more detail in the

following sections on design of the apparatus. The numerical results are contained in Appendix B, together with similar calculations for the other reactions mentioned above which might be simultaneously studied in a tagged, unseparated beam.

In the next section, we discuss the design of a spectrometer to measure the decay products of the ρ sufficiently accurately to determine the invariant mass of the pion pair, and also to determine the invariant mass of the resonance produced at the target vertex. It is, however, still necessary to measure at least the directions of the decay products of the baryon resonance because the correlations between the alignments of the two resonances yield important information concerning the reaction mechanism. In the two succeeding sections, we consider first a liquid hydrogen target with wire chambers and Cerenkov counters, and second a rapid-cycling bubble chamber, as alternative methods for measuring the decay of the resonance which is produced at low momentum in the laboratory.

III. THE DOWNSTREAM SPECTROMETER

The apparatus described below is designed to accept all events of reaction (1) for $p_{beam} = 50$ GeV/c and $-t(p \to \Delta) < 1.2$.

Dimensions

The accuracy required is set by the requirement that the Δ mass be determined to better than 60 MeV by a measurement of the products of the ρ decay. This sets the accuracy of the beam to $\Delta p/p \simeq 0.1\%$ and the ρ momentum must be measured to ~ 50 MeV/c. The ρ momentum for the range of $|t|$ values considered here varies from 49.6 to 49.0 GeV/c. However, as can be seen from Figs. 2 and 3, the ρ decay can be very asymmetric, with the resultant pions ranging from 1.7 to 47.9 GeV/c in momentum. The downstream spectrometer is thus of two-stage design. The first stage measures π momenta from 1.7 to 18 GeV/c and the second from 18 to 50 GeV/c. Figure 4 and Table I give some of the relevant dimensions.

Wire planes with magnetostrictive readout are used. Each plane in Fig. 4 consists of two x-y planes and each arm of the spectrometer has an additional w-plane to resolve ambiguities. Magnetostrictive readout is known to give problems in magnetic fields. For this reason no plane is situated closer than 0.5 m to the magnets of the spectrometer, so that adequate shielding can be provided. Planes p_1 through p_4 measure momenta from 1.7 to 10 GeV/c. If it were not for p_4, p_5 could catch all the low momentum particles only if it were excessively large. Another advantage of p_4 is that the lowest momenta particles can be measured with the lowest multiple scattering possible. The counter hodoscope C_1 contributes multiple scattering only to the measurement of the higher momenta, where its effect is less important.

Table I. Dimensions of Downstream Spectrometer.

(See Fig. 4 for a definition of the symbols.)

Space	Length (m)	Wire Plane	Horizontal × Vertical Dimension (m×m)
L_1	4	B_1	0.02×0.02
L_2	0.5	B_2	0.02×0.02
L_3	0.5	p_1	0.06×0.06
D_1	4	p_2	0.55×0.55
L_4	0.5	p_3	3.4 ×0.92
M_1	2	p_4	5.08×1.04
L_5	0.5	p_5	2.48×1.53
D_2	1	p_6	2.6 ×1.47
D_3	4	p_7	3.80×1.93
L_6	0.5		
M_2	4		
L_7	0.5		
D_4	5		

Counter	Horizontal × Vertical Dimension (m×m)	Magnet	Field (kG)	Length × Width × Height (m × m × m)
G_1	4×4 (outside)	M_1	20	2×2.32×0.86
G_2	4×4 (outside)	M_2	40	4×2.40×1.45
G_3	3.6×2.0			
C_1	5.08×1.04			
C_2	3.80×1.93			

Planes p_1, p_2, p_3, and p_5 form the spectrometer to measure momenta in the range 10 to 18 GeV/c and planes p_3, p_5, p_6, and p_7 cover the range 18 to 50 GeV/c. The direction of the magnetic fields has been reversed to reduce the aperture of the second magnet.

The apertures of the magnets, the sizes of the wire planes, and the spacings between them were decided by tracing through on the computer a series of pions of momenta and production angles with limits given by the curves of Fig. 2. The spectrometer will accept all angles and momenta of the pions from the ρ decay.

The downstream spectrometer is over-designed in the sense that no loss of events in azimuth has been allowed. The horizontal apertures have been designed to allow the lowest momentum particles produced at their maximum angle, on either side of the beam, to pass through the first magnet even if they are defocused by this magnet. A relaxation of this restriction, either by demanding it only for low-momentum

particles produced at one side of the beam or by demanding that only focused particles be accepted by the spectrometer will reduce these apertures. The vertical apertures can also be reduced as, for example, was suggested by Meyer[6] in his design. These methods may reduce the apertures with a sacrifice of rate and an introduction of experimental bias. A complete optimization has not been carried out, but a reduction of up to a factor of three or so in the magnetic volume would appear to be acceptable. Similar remarks can be made about the downstream magnet, although the saving in horizontal aperture will be less because of the greater rigidity of the particles measured in this magnet.

Further reduction in the aperture of the magnets could also be achieved if one is prepared to throw away the pions of lowest momentum. This solution is not very attractive for an experiment which aims to investigate fully the angular distribution and the density matrix elements. For example, Fig. 5 shows that if only pions above 5 GeV/c are accepted for measurement, about 25° in the center-of-mass of the ρ in the forward and backward directions are lost. This loss is particularly severe for the ρ with a $\cos^2$ decay distribution. However, this solution is acceptable if the bubble chamber is used in place of the hydrogen target (see Section V).

Figure 6 shows that for a pion of 4.5 BeV/c, $\Delta p/p$ is about 1.25% or $\Delta p \simeq 50$ MeV/c and $\Delta\theta$ is about 1.25 milliradians. If one could be satisfied that measurement of π's below about 5 BeV/c would be done in the system surrounding the target, the downstream spectrometer would only have to deal with pions above this momentum. In this case the horizontal aperture of the first magnet can be immediately reduced to 1.30 m as opposed to 2.32 m. There is, of course, a corresponding decrease in the size of planes p_3, p_4, and in the counter hodoscope C_1.

Vetoes and Triggering

The downstream veto counters are lead-lucite Cerenkov counters to detect gamma-ray showers from the decay of π^o's which have not been detected in the upstream counter box. These counters would be set with a threshold high enough not to count single minimum ionizing particles. G_1 and G_2 cover the faces of the two magnets, and G_3 covers the γ's which have traveled the length of the spectrometer.

C_1 is a hodoscope to count the number of particles downstream to aid in obtaining a tight trigger. For the purposes of calculation of errors (see the next section), it has been assumed that it is made of 1/4 in. thick scintillator. Since the multiple scattering caused by such a counter is acceptable only at the higher pion momenta, it must be placed behind p_4 and thus be of large size. It can be either a picket fence with vertical components (x counters), 5 m long and 700 cm high, or it can be a set of crossed x and y counters with the y counters consisting of two 2.5 m

horizontal lengths. A detailed study would have to be undertaken to find the type and dimensions of this counter. However, it appears to pose rather a formidable construction and logic problem. The state of the art of wire chambers run in the proportional mode may have progressed sufficiently to allow such chambers to be used as hodoscopes. Their low density and high resolution would allow their use much closer to the target.

C_2 is a large sheet of scintillator, or several large counters to detect a charged particle going through the spectrometer. Figure 3 shows that at least one pion from the ρ decay always has momentum greater than 18 BeV/c and will traverse the spectrometer. C_1 and C_2 are 1/4 in. of plastic scintillator in the beam direction. The dimensions of G_1, G_2, G_3, C_1, and C_2 are given in Table I. A downstream trigger is then provided by $\bar{G}_1 \bar{G}_2 \bar{G}_3 [C_1(i) C_1(j)] C_2$.

Measurement Accuracy

The actual errors in momentum and angle measurements arising from resolution in the wire planes, and multiple scattering in the material traversed by the particles have been calculated using the formulas given in Apendix A.1.

These errors were put into the ray tracing program to give the overall $(\Delta p/p)$ for each momentum. To keep the multiple-scattering errors in the arms to the order of that caused by the planes and the counter hodoscope the spectrometer should be filled with helium bags. The momentum accuracy actually achieved when consideration of all these errors is included is shown in Fig. 7 and listed in Table II for some representative cases. The breaks in the curves of Fig. 7 arise from the fact that different momenta are measured in different planes as described above. The angle error calculation does not include multiple scattering in the hydrogen target, which becomes important only in the measurement of the production angles of pions of less than 10 GeV/c. It does not, of course, affect the measurement of momenta.

It is important to discuss whether this multiple-scattering error (which is ~ 0.7 mrad for the lowest momentum) makes the measurement of the mass of the ρ unacceptably inaccurate. The discussion in Appendix A points out that the opening angle between the two pions must be measured to a precision of 4% to achieve the design accuracy. It is clear from Table II that, apart from the most asymmetric decays, this accuracy has been achieved. For the decays in which one pion has less than 10 GeV/c, it turns out that the approximation used in Appendix A ($m_\rho^2 \sim p_1 p_2 \alpha^2$) which gave this figure of 4%, becomes very poor. (It is clearly wrong for $\alpha \sim 0$.) A brief calculation for specific cases shows that changes in the opening angle of as much as 2 mrad causes a change in the ρ mass by values ranging from ~ 30 to ~ 5 MeV, as the opening angle ranges from 2° to 0°.

Thus it appears that this experiment can measure ρ decays down to the smallest angle. In fact the ultimate limitation is the fact that two tracks are not resolved if they are separated by less than ~ 2 mm in the wire plane. This means that since the first plane is 0.5 m away from the target, pions with angles of less than 4 mrad, or 0.23° in the laboratory cannot be measured. Figure 8 shows, however, that this accounts for only 2° in the center-of-mass angle of the ρ in the direct forward and backward direction. Since the particles will be separated by the magnet [very greatly since the pion momenta are very different for small opening angles (see Fig. 9)], these events will cause a good trigger and will be acceptable events. The fact that the particles are indistinguishable places them in the correct center-of-mass angular bin, and the arguments above show that the ρ mass can be adequately measured for the smallest opening angles.

IV. TARGET AND COUNTERS

Rates

The primary advantage of a liquid hydrogen target and counter wire-chamber system for measuring the decay of the Δ is that a higher rate can be achieved than is possible with a fast-cycling bubble chamber. For the purposes of discussion consider three cross sections:

1. σ(4-prong)--the cross section for four-prong events. This is extrapolated to be ~5 mb at 50 BeV/c (based on 8 mb at 20 BeV/c quoted by K. Strauch[5]).

2. σ_{trig}--the constrained trigger cross section. This cross section should be somewhat smaller than σ(4-prong) if π^o's are vetoed and one slow particle is required.

3. σ_{event}--the actual cross section for rho production with an N^*. This is taken to be 46 μb for reaction (1) and 5 μb for reaction (2). (At 20 GeV the cross section is 50 μb to the state $N^{*o} + \pi^+ + \pi^-$.)

If the efficiency is 1.0 the rates are set by the length of the target and the beam rate. A target length of 10 cm gives a multiple-scattering angle of ~ 0.7 mrad at 2 BeV/c. As is discussed above, this is consistent with the required ρ mass resolution. The diameter of the target could be as small as 2 mm and still accommodate the beam spot. Effectively 4π solid angle for the target could be obtained by hanging it on a long fill tube. With a target spot of 2 mm, it should be possible to limit the beam divergence to 0.5 mrad. If a smaller effective divergence is required the beam particles could be tagged in a counter hodoscope at the exit of the last quadrupole thus defining the direction of each beam particle more precisely. A beam of 10^5/pulse can probably be used without desensitizing the planes in the beam region. Somewhat higher beam rates would require more sophisticated techniques such as desensitizing or using proportional wires in the region of the beam. For this intensity, there are

Table II. Representative Errors in Measurement of Angles and Momenta of Pions in Downstream Spectrometer for a ρ Momentum of 49.6 GeV/c (corresponding to $t \approx t_{min}$). The Angle Errors Do Not Include the Effects of Multiple Scattering In the Hydrogen Target (See Text).

Laboratory Opening Angle of Decay Pions α mrad	First Decay Pion: Laboratory Momentum p_1 (GeV/c)	First Decay Pion: Error in Momentum δp_1 (MeV/c)	First Decay Pion: Error in Angle $\delta\theta_1$ (mrad)	Second Decay Pion: Laboratory Momentum p_2 (GeV/c)	Second Decay Pion: Error in Momentum δp_2 (MeV/c)	Second Decay Pion: Error in Angle $\delta\theta_2$ (mrad)	Error in ρ Momentum δp_ρ (MeV/c)	Error in Opening Angle $\delta\alpha$ %
0	47.9	55.0	0.12	1.7	2.5	0.36	55.1	1.21
41.6	45.4	49.0	0.12	4.2	10.0	0.49	50.0	1.27
35.8	41.1	41.3	0.12	8.5	26.0	0.44	48.8	0.84
35.0	39.5	38.0	0.12	10.1	23.8	0.27	44.8	0.77
31.1	34.0	30.0	0.12	15.6	39.5	0.21	49.6	0.72
29.6	30.0	24.5	0.13	19.6	11.5	0.17	27.1	0.69
27.5	24.8	18.9	0.14	24.8	18.9	0.14	26.7	0.72

200 four-prong events per pulse and 0.2 $\rho^{o}\Delta^{o}$ events per pulse, or 5×10^{3} true events per day.

If $\sigma_{trig} = \sigma$(4-prong), the trigger rate is barely tolerable. Core-memory chambers can be fired every millisecond, and 200 events of this complexity could be read into a computer, but not fully analyzed, every pulse. A more comfortable rate might be 40 events/pulse, which could be handled by magnetostrictive readout systems and would allow complete computation at a level of 100 msec/event. This would require a trigger condition that eliminated four-fifths of the four-prong events.

The Target System

The purposes of the counter wire-chamber system surrounding the target are threefold:

1. To measure the angles of the two charged particles from the decay of the Δ
2. To distinguish the proton from pion whenever a kinematic ambiguity exists
3. To improve the trigger provided by the downstream spectrometer.

Angle Measurement

The kinematics program described above gave values of lab momenta and angles for the decay products of the Δ for given center-of-mass decay angles and production t values.

Only a reasonably coarse measurement of the angles is required since the maximum complexity for the angular distribution of the decay of a spin 3/2 particle is $a + b\cos^{2}\theta$. Furthermore, it can be seen from the plots of decay kinematics in Fig. 10 that at least up to $-t = 0.8$ GeV^{2} the pions are emitted into the full solid angle, and thus the lab angles are not sufficiently distorted to demand high angular resolution in order to map the center-of-mass decay distribution.

The simplest system for the angle measurement is a set of wire planes. Each set of wire planes will form a box of square cross section surrounding the target (see Fig. 11). The inner box will be made up of planes 14 cm long by 5 cm wide. The wires will be 5 cm long with 1 mm spacing and will define the interaction point in the liquid H_{2}.

The top plane is made in 3 sections to fit around the fill tubes and ancillary equipment. A set of four larger planes 30 cm wide by 38 cm long, each with a set of wires parallel to beam and a set perpendicular to the beam will define the angle of each track.

Measurement of the angles of two outgoing slow particles as well as the angles and momenta of the two fast pions overconstrains the event. If there are no neutral particles a two-constraint fit is possible. This will in general identify the pion and proton. Interchanging the assignments will lead to an energy unbalance unless the two particles have approximately equal momenta.

Misidentification

In Fig. 12, we have plotted the magnitude of the pion momentum vs the magnitude of the proton momentum for all the t values used in the kinematic calculations. With the accuracy of the downstream spectrometer which is described in the previous section, misidentification of the pion and proton tracks can only occur if $|\vec{p}_p| - |\vec{p}_\pi| \lesssim 50$ MeV/c. The area where this relation is satisfied is shaded in Fig. 12. The pion and proton momenta at the extremes of this region are approximately 0.25 and 0.55 GeV/c. For pions, β is ≥ 0.85. For protons, β varies from 0.27-0.5. Thus pions and protons can clearly be distinguished by means of a set of water Cerenkov counters surrounding the downstream half of the outer wire planes. It is unnecessary to cover the backward hemisphere since the kinematics show that only pions can reach lab angles $> 90^\circ$.

For small values of t the angles for which $\vec{p}_\pi$ and $\vec{p}_p$ are roughly equal result in a pion and proton on opposite sides of the beam and a simple arrangement of Cerenkov counters will suffice. For larger values of t, the two particles tend to move in nearly the same direction and reasonably good spatial resolution in the Cerenkov counters is required. It should be noted however that if the slope $\ell n\ (d\sigma/dt)$ vs t, which was observed to be > 11 at 8 GeV/c (Ref. 4), persists to our energies, then over 65% of the cross section occurs for $|t| < 0.1$. A thin (~1/4 in.) scintillation counter should be placed in front of each Cerenkov counter to provide a coincidence pulse to eliminate noise in the Cerenkov counter.

The ends of the wire-chamber enclosure boxes should be covered by wire planes with holes in them sufficiently large to avoid the incoming beam and matched to the angular acceptance of the magnetic spectrometer. Slow particles which pass through this hole will be detected in the first two planes of the downstream spectrometer.

Finally, improved triggering is obtained by demanding one or two pulses in the scintillators in front of the Cerenkov counters and by surrounding the entire box except for the entrance and exit holes with gamma veto counters of the type described in the previous section.

It may be noted that for values of t very near t_{min} and for 0° or 180° decay of the Δ it is possible for both charged particles to leave the target box through the downstream spectrometer exit hole. If we demand a count in our target counters as part of the trigger, this will introduce a bias in the angular distribution. However, in this configuration one of the particles is always of very low momentum and will be swept into the yoke of the first spectrometer magnet. Thus a pulse in a scintillation counter covering the face of the yoke can be used as an alternative to a pulse in one of the scintillators of the largest array in defining the master trigger.

V. DOWNSTREAM SPECTROMETER WITH A BUBBLE CHAMBER AS TARGET

Description

Complete observation of the process

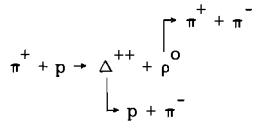

can be carried out by replacing the hydrogen target with a rapid-cycling hydrogen bubble chamber. Although it is beyond the bounds of any existing system, it seems not too rash to assume that a chamber 1 meter in diameter and 50 cm deep could be made to cycle 100 times per second and still yield accuracy of track position determination (~80 microns) comparable to existing chambers of its size (for this accuracy a large front window is assumed). It is quite reasonable to assume a magnetic field of 40 kG for the chamber. The outer diameter of the chamber, using usual construction methods, would probably be about 1.5 meters, coaxial with the chamber itself. Farther out along the axis, space would be needed for the expansion mechanism and the lighting and photographic equipment. Thin windows (total material ≈ 1/8 in. stainless steel) for the incident beam and the outgoing secondary particles nearly along the beam line would be provided. In other directions secondaries would traverse considerably more material (about 3/4 in. stainless steel on the sides, 2 in. of glass on the top, 1 in. stainless steel on the bottom) before they could be detected by auxiliary counters or spark chambers outside the bubble chamber.[7] The kinematics for a 50-BeV bombarding π^- (see Fig. 10) show that the decay proton in the desired events will have less than 1.5 BeV/c momentum and will always be within 67° of the beam direction for $|t| < 1.2$ (GeV/c)^2. The pion from the Δ decay can go in any direction and has quite low momentum, always less than 1 GeV/c. When it lies in the backward hemisphere, it has extremely low momentum (less than 100 MeV/c) and will in many such cases stop in the bubble chamber.

Consider the accuracy with which one can determine that the desired event $\Delta + \rho$ has occurred. Figure 6 shows curves for $\Delta p/p$ in % and $\Delta\theta$ in mrad for a field of 40 kG. The accuracy of momentum measurement is about 3/4% for the π and the proton and will not contribute appreciably to the error in the calculated invariant mass of $p\pi^-$. Multiple scattering in the hydrogen dominates the angular error for these low momentum particles, but again considering that the angles themselves are large (of the order of radians) the identification of the Δ is clear. Putting this information on the slow particles together to determine whether or not a ρ has been

formed (without looking at the $\pi^+\pi^-$) is more difficult because of the uncertainty in the exact mass of the Δ and the uncertainty in its angle with respect to the beam. Since the downstream spectrometer is designed to have precision sufficient to determine that a ρ was formed with a Δ, it is assumed that this feature will be retained and the bubble chamber used primarily to verify that the event consists of 4 charged prongs with a π^+ and proton produced as a Δ, and to identify the proton with certainty by bubble density. As has been discussed earlier, the bubble chamber's ability to measure the low-momentum decay pions from the ρ makes it possible to relax some of the requirements on the downstream spectrometer. In particular one would not need to cover such a wide angle behind the upstream magnet.

Rates

With no special lateral beam stepping through the chamber, one should probably limit the beam load to about 20 tracks per expansion or 2,000 per pulse. Assuming 80 cm per beam track (for σ_{total} = 25 mb), a total of 1.5 interactions per expansion or 150 per accelerator pulse is expected. In general, with the electronic trigger, it should not be difficult to decide which event in the chamber corresponds to the triggering tracks nor should it be difficult to see clearly the desired secondary tracks. Finally, the desired events with ρ and Δ occur at the rate of about 1 every 3,300 expansions or 1 per 33 accelerator pulses. The following points should be noted:

1. Roughly 1,000 desired events per day could be collected with such an apparatus.

2. Whereas it would be out of the question to take a photograph on even half of the expansions, it would be quite efficient to introduce 1 or 2 additional triggers for events giving rates similar to the $\rho\Delta$ rate, by triggering on incoming K's, for example.

3. This apparatus probably would operate on a modest (< 20%) fraction of the circulating proton beam and consequently should be compatible with a relatively large number of other experiments.

4. It is important to consider in detail what alternative reactions would be well measured in this apparatus.

Triggering and Background

There is a veto counter for π^o's (γ's) at the very end of the downstream spectrometer, and the front of each magnet is covered. As many veto counters for π^o's are placed around the bubble chamber as is practicable. It is assumed that these latter will be only about 35% effective, but they will still be a major help in reducing the total number of pictures. The trigger will consist of detecting 2 and only 2 fast particles in the downstream spectrometer. The total cross section for events with 4 charged particles at 50 BeV/c (including those with additional secondary π^o's) is

estimated to be 5 millibarns based on the numbers given by K. Strauch[5] at 20 BeV/c. Roughly, we assume about 5% will correspond to $\pi^- p \pi^+ \pi^-$ with nothing missing and an equal number of events with a single π^o; the remaining 90% have more than one π^o. It is reasonable to assume that the events with more than one π^o will ordinarily set off one of the veto counters, assuming 98% efficiency for detecting at least one of four gamma rays. Most of the two-pronged events (e.g. elastic scattering) will leave one particle too slow to penetrate the downstream spectrometer; assume ~1% could trigger the system. The events with 6 prongs or more will usually correspond to a fast forward "fireball" or equivalent which would tend to put more than two fast charged particles through the downstream spectrometer. Combined with this is the enhanced likelihood that there will be one or more gamma rays setting off a veto counter. Assume only 1/3% of these events will trigger the system. Table III summarizes the resulting trigger rates and evaluates the triggering signal-to-noise ratio. The resulting signal-to-noise ratio is not high but places this experiment in the category of bubble-chamber experiments of the past done without triggering, tagging, or labeling of any kind; i.e., 50,000 pictures yield 1,000 final relatively unbiased examples of the process to be studied.

Table III. Trigger Rate.
(Two Fast Charged Particles With No Gamma Rays Detected)

Total Cross Section 25 mb

Name	Cross Section (mb)	Trigger Probability, %	No. of Triggers per Accelerator Pulse
A. Background Leakage			
Two-Pronged Events (mostly elastic scattering)	5	1	0.3
More than 4 Prongs	15	1/3	0.3
4-Pronged Events Accompanied by γ's	4.75	2	0.6
B. Signal-like Background			
4-Pronged Events with no Missing Neutrals	0.25	98	1.5
C. Signal			
$p\Delta$	0.005	98	0.03

Total estimated triggers: 2.8/pulse

$$\text{Triggering } \frac{\text{Signal}}{\text{Noise}} \sim \frac{\text{Signal } 0.03}{3} \sim \frac{3}{280} \text{ or } \sim 1\%$$

Every picture would contain some event, and approximately one-half of the events would be measured in making the selection of the $\Delta\rho$ events. It is believed that the estimated rates and efficiencies used to construct Table III are conservative. Efforts would be made to improve the signal-to-noise ratio. However, the situation described is satisfactory for the objective of studying the details of $\Delta\rho$ production at 50 BeV.

Triggering on Different Beam Particles

In the last section it was assumed that the beam would be sufficiently pure that beam contamination would not contribute significantly to the background and that normal bubble-chamber measurement and analysis procedures would sort out the desired events. With a modest hodoscope in front of the chamber and threshold Cerenkov counters the individual beam particle producing an event could be labeled as π^+, K^+, or p. If an experiment similar to the one described here were run at the early stages of NAL operation, such a labeling procedure in an unseparated beam would seem to be the ideal way in which to obtain several low-rate, but interesting, processes in the same operation. This has not been looked at in detail but seems much more likely to be interesting than trying to prepare auxiliary triggers for unusual events initiated by π^+. For example, certainly the process:

$$K^+ + p \rightarrow K^{o*} + \Delta$$

followed by

$$K^{o*} \rightarrow K^+ + \pi^-$$

$$\Delta \rightarrow p + \pi^+$$

must be detectable in this apparatus, and it would make an interesting study.

By-Products

Most of the 4-pronged events would ultimately be measured and consequently we would see anything new or dramatic in that fraction with zero or one missing neutral (about 10% of all 4-prongs, which from Table III are about 60% of all triggered photographs). It seems likely that one would make a brief study of a sample of the 6-pronged events, concentrating on the ones which had no missing neutrals. Such 4-constraint events would have been greatly concentrated by the veto counters' detection of π^o's. Although it would be a biased sample, a selection of these events with the proton identified by bubble density could yield interesting new results even with a small number of events.

Finally, from a long run, there would be a reasonable number of events in which strange particle production occurred and which were readily identifiable in the bubble chamber. These could prove to be of major interest.

VI. CONCLUSIONS

We have presented the design of a high precision spectrometer to measure the reaction $\pi p \rightarrow \rho\Delta$ at 50 BeV/c. Although some of the equipment is expensive, the experiment can certainly be done with existing techniques and thus is a candidate for a first-round experiment at NAL.

The use of two large magnets is necessary to achieve the accuracy required. We have made no attempt to estimate the cost of the system we propose. This should certainly be done. As mentioned in the text, various methods could be used to reduce the size of the magnet apertures, and thus their cost. Since similar arguments will apply to every magnet NAL will build, a study should be carried out to determine whether it is more costly to reduce all magnet apertures or to accept the loss in rate and larger running times which will thus result.

It is clear that the use of a bubble chamber as a target has some distinct advantages. The distinction between the low momentum proton and pion for example, which is not simple to do with counters, is achieved trivially. This ability of the bubble chamber is likely to be of equal value in the study of all reactions which proceed by processes which give small momentum transfer to some of the final-state particles. There is clearly some point at which the product of cycling rate and cross section makes the use of a medium-sized bubble chamber rather inefficient. For this reason, we feel it is important that NAL support the present effort in the development of the rapid-cycling chamber.

Since it remains true that the bubble chamber is better at the survey of a large number of channels, rather than a high-statistics investigation of a particular one, and since this property will be most valuable in the first few years of NAL operation, we feel that NAL should seriously consider the possibility of having a medium-sized, rapid-cycling chamber available close to beam day. It is clear from this and other studies that a field of close to 40 kG is necessary to achieve sufficient accuracy on the measurement of $\lesssim 10$ GeV/c particles, for a chamber of modest dimensions.

We have not investigated the possibility of doing this experiment with a streamer chamber at the target. It would be valuable to study this question for the purposes of comparison.

As discussed in the text, the present system will undoubtedly be able to study a variety of other reactions over a range of energies. A systematic study of the flexibility of this and other systems proposed at the summer study would be of great assistance in deciding on a specific system.

APPENDIX A. CALCULATION OF ERRORS FOR DOWNSTREAM SPECTROMETER

It is the intention of this experiment to measure the mass of the Δ, produced in the reaction $\pi p \rightarrow \rho\Delta$, to ~60 MeV, by measuring the momentum of the forward-produced ρ in the downstream spectrometer. Section 1 of this appendix presents the details of the calculations used to set the approximate limits of accuracy on angle and momentum measurements required to satisfy this condition, and section 2 details the formulas used to calculate the actual measurement errors caused by resolution and multiple scattering.

1. In the reaction $\pi p \rightarrow \rho\Delta$, the mass of the Δ, treated as missing, is given by

$$M_\Delta^2 = (E_\rho - E_\pi - m_p)^2 - (\vec{p}_\pi - \vec{p}_\rho)^2, \tag{1}$$

with an obvious notation. Then the error in M_Δ^2 may be estimated by considering

$$\delta M_\Delta^2 \simeq \delta m_\rho^2 + \delta p_\pi (2m_p - p_\rho \theta^2) - \delta p_\rho (2m_p + p_\pi \theta^2) - 2\theta\, p_\rho p_\pi \delta\theta, \tag{2}$$

where θ is the production angle of the ρ. The approximations $E_\pi = p_\pi$, $E_\rho = p_\rho$ (which are very good since p_π is 50 GeV/c and $p_\rho > 49$ GeV/c for the t range considered), and $\cos\theta = 1 - \theta^2/2$ (good for even the maximum production angle of ~ 20 mrad) have been made. To substitute the momenta of the pions from ρ decay into (2) leads to an excessively complicated formula. Accordingly, the following assumptions have been used. Since

$$p_\rho \theta^2 \sim p_\pi \theta^2 \sim 50 \times (20 \times 10^{-3})^2 \sim 0.02 \text{ GeV} << 2m_p,$$

(2) simplifies to

$$\delta M_\Delta^2 \sim \delta m_\rho^2 + 2m_p (\delta p_\pi - \delta p_\rho) - 2p_\rho p_\pi \theta\ \delta\theta. \tag{3}$$

As discussed in the text, the angular error on the faster pion from the ρ decay is ~0.1 mrad. Since it will be the direction of the faster pion which will dominate in the calculation of the ρ direction and since the incident beam angle can be defined upstream to a similar precision, it is reasonable to expect that $\delta\theta$ will be conservatively ~ 0.3 mrad; therefore

$$2p_\delta p_\pi \theta\delta\theta \leq 2 \times 50 \times 50 \times 0.3 \times 10^{-3} \times 20 \times 10^{-3} \sim 0.03 \text{ GeV}^2.$$

If the errors in the beam and ρ momentum are 0.1%, the contribution to δM_Δ^2 is 0.09 GeV^2 from each. If δM_Δ has to be ~60 MeV, $\delta M_\Delta^2 \sim 0.14\ (\text{GeV})^2$, and a limit of $\delta m_\rho^2 \sim 0.05$ is set assuming all the errors in (3) are uncorrelated. This means that

the ρ mass must be determined to ~ 30 MeV. It is given by

$$\begin{aligned} m_\rho^2 &= (E_1 + E_2)^2 - (\vec{p}_1 + \vec{p}_2)^2 \\ &= m_1^2 + m_2^2 + 2E_1E_2 - 2p_1p_2 \cos\alpha \\ &\simeq m_1^2 + m_2^2 + p_1p_2\alpha^2, \end{aligned} \tag{4}$$

where 1,2 refer to the two pions from the decaying ρ, and α is the angle between them. In the last step of (4) the approximations $E_1 = p_1$, $E_2 = p_2$, $\cos\alpha = 1 - \alpha^2/2$ (α is always $\lesssim 2.5^\circ$), have been made.

Then,

$$\delta m_\rho^2 \simeq p_1\alpha^2\,\delta p_2 + p_2\alpha^2\,\delta p_1 + 2p_1p_2\,\alpha\delta\alpha.$$

Therefore,

$$\frac{\delta m_\rho^2}{m_\rho^2} \simeq \frac{\delta p_1}{p_1} + \frac{\delta p_2}{p_2} + 2\,\frac{\delta\alpha}{\alpha}. \tag{5}$$

It is now necessary to discuss the errors in p_1 and p_2. Now

$$\vec{p}_\rho = \vec{p}_1 + \vec{p}_2,$$

and

$$p_\rho^2 = p_1^2 + p_2^2 + 2p_1p_2\cos\alpha,$$

where 1,2 refer to the pions from the ρ decay and α is the angle between them. Therefore

$$p_\rho^2 \simeq (p_1 + p_2)^2 - p_1p_2\alpha^2. \tag{6}$$

Now Fig. 3 and the tables in Appendix B show that $(p_1 + p_2)$ is always within 0.1 GeV/c or so of 50 GeV/c. Since $\alpha^2 \lesssim (40\times10^{-3})^2 \simeq 1.6\times10^{-3}$ and the maximum of p_1p_2 occurs when $p_1 = p_2 = 25$, then $p_1p_2\alpha^2 \lesssim 1 << (p_1 + p_2)^2$. Thus $p_\rho = p_1 + p_2$ to a good approximation. This implies two things:

1. Roughly $\delta p_\rho = \sqrt{(\delta p_1)^2 + (\delta p_2)^2}$, so that the highest momentum pions must be measured to about 0.1% to give this accuracy in p_ρ: for $p_1 \simeq p_2 \simeq 25$ GeV/c, for example, $\delta p_1 \simeq \delta p_2$ must be ~35 MeV/c, or ~0.14%.

2. The error in the opening angle α has, to first approximation, little effect on determining p_ρ.

Returning to (5), since $\delta m_\rho^2/m_\rho^2$ has already been determined to be ~0.08, the errors in p_1 and p_2 already set make little contribution. Thus the allowable error on the determination of α is approximately 4%.

2. The error in measuring momentum is given by

$$\frac{\Delta p}{p} = \frac{p\delta\theta}{0.03B\ell} \tag{1}$$

where

p is the momentum in GeV/c, and Δp is its error,

B is the magnetic field in kG,

ℓ is the length of the magnet in meters.

$\delta\theta$ is given by

$$\delta\theta = \sqrt{\delta\theta_1^2 + \delta\theta_2^2}, \tag{2}$$

where

$\delta\theta_1$, the multiple scattering error, is given by

$$\delta\theta_1 \simeq 0.015\sqrt{t}/p. \tag{3}$$

Here t is the thickness of material traversed, in radiation lengths. $\delta\theta_2$, the measuring error, is given by

$$\delta\theta_2 = \delta\left[2(1/D_1^2 + 1/D_2^2)\right]^{1/2}$$

where D_1 and D_2 are the lengths of the lever arms on either side of the magnet.

The values used for the various constants in the calculations of these errors are listed in Table IV.

It is also important under some circumstances that the spectrometer have good resolution in -t, the momentum transfer squared. This is true, for instance, for investigations of "conspiracy."

$-t \simeq (\bar{p}\bar{\theta})^2$ where $\bar{p}$, $\bar{\theta}$ are laboratory quantities for the ρ. Then,

$$\frac{\delta t}{t} = 2\frac{\delta\bar{\theta}}{\bar{\theta}} + 2\frac{\delta\bar{p}}{\bar{p}}.$$

Let

$$\frac{\delta\bar{p}}{\bar{p}} = \sqrt{2}\,\frac{\delta p_{\pi_1}}{p_{\pi_1}} = \sqrt{2}\cdot 10^{-3}$$

(i.e., 0.1% momentum resolution on the individual particles).

$\bar{\theta} = 1.2 \cdot 10^{-2}$ radians for t = -0.4.

Assuming a $\delta\bar{\theta}$ of 0.5 milliradians

$$\frac{\delta t}{t} = \frac{1.0 \cdot 10^{-3}}{1.2 \cdot 10^{-2}} + \sqrt{2} \cdot 10^{-3}.$$

Thus the angular resolution dominates the determination of t and it seems easy to obtain 10% measurements with the angular resolution of the downstream spectrometer.

APPENDIX B. KINEMATICS FOR THE PROCESS $\pi + p \rightarrow \Delta + \rho$ WITH DECAY OF THE UNSTABLE PARTICLES

Kinematics were generated for the process

$$\pi + p \rightarrow \rho + \Delta$$
$$\rho \rightarrow \pi + \pi \qquad \Delta \rightarrow \pi + N$$

using the basic program DECPRO. For a given set of masses the program calculates the momenta and direction in the laboratory of all four outgoing particles with the decay angle of the original unstable particles ranging over six angles in the center-of-mass. It can do this over a range of -t values (extending from the minimum -t) or center-of-mass angles.

For the tabulations here the masses used were

π	+	p	$\rightarrow$	ρ	+	Δ
(0.139)		(0.938)		(0.760)		(1.238)

ρ (particle 1) (0.760) $\rightarrow$ $\pi_1 + \pi_2$ (0.139)(0.139)

Δ (particle 2) (1.238) $\rightarrow$ $\pi_1 + p_2$ (0.139)(0.938)

All momenta (BeV/c) and angles (degrees) are in the laboratory except where explicitly stated. T stands for momentum transfer squared.

The kinematics for several other processes are also given. The incident beam momentum is tabulated in the upper right hand corner. In all cases decay particle 1 is the meson. In the Δ case the pion is p_1 etc.

A. $\pi + p \rightarrow \rho + \Delta$ 50 GeV/c

$\rho \rightarrow \pi + \pi$ $\Delta \rightarrow \pi + p$

```
********************
 ACM   ALAB            PLAB            TLAB            BETA-GAMMA
 0     0               49.6443         48.8901         65.3214
       0               .355714         5.00903E-03     .28733
            T(T TØ B)= -3.96932E-03
       DECAY ØF PARTICLE NØ.  1  (ACM,P1,P2,A1,A2,A12)
    0       47.927      1.718          .00      .00        .00
   45       41.160      8.488          .35    -1.69       2.04
   90       24.825     24.825          .82     -.82       1.63
  135        8.488     41.160         1.69     -.35       2.04
  180        1.718     47.927          .00      .00        .00
       DECAY ØF PARTICLE NØ.  2  (ACM,P1,P2,A1,A2,A12)
    0         .321       .035          .00      .00        .00
   45         .299       .196        33.45   -57.22      90.67
   90         .246       .363        71.50   -40.02     111.52
  135         .190       .479       119.57   -20.15     139.72
  180         .165       .520       180.00     -.00     180.00
********************
 ACM   ALAB            PLAB            TLAB            BETA-GAMMA
 1.51524  .145179      49.6357         48.8816         65.3102
      -19.0407         .385512         5.86355E-02     .311399
            T(T TØ B)= -2.00002E-02
       DECAY ØF PARTICLE NØ.  1  (ACM,P1,P2,A1,A2,A12)
    0       47.919      1.717          .15      .15        .00
   45       41.153      8.487          .49    -1.54       2.04
   90       24.820     24.820          .96     -.67       1.63
  135        8.487     41.153         1.83     -.20       2.04
  180        1.717     47.919          .15      .15        .00
       DECAY ØF PARTICLE NØ.  2  (ACM,P1,P2,A1,A2,A12)
    0         .329       .057       -19.04   -19.04        .00
   45         .306       .209        13.62   -71.15      84.77
   90         .248       .381        51.03   -56.81     107.84
  135         .187       .502        99.09   -38.23     137.32
  180         .160       .545       160.96   -19.04     180.00
********************
 ACM   ALAB            PLAB            TLAB            BETA-GAMMA
 2.27172  .217676      49.6251         48.8709         65.2962
      -26.6739         .419977         6.92965E-02     .339238
            T(T TØ B)= -4.00003E-02
       DECAY ØF PARTICLE NØ.  1  (ACM,P1,P2,A1,A2,A12)
    0       47.908      1.717          .22      .22        .00
   45       41.144      8.485          .57    -1.47       2.04
   90       24.815     24.815         1.03     -.60       1.63
  135        8.485     41.144         1.91     -.13       2.04
  180        1.717     47.908          .22      .22        .00
       DECAY ØF PARTICLE NØ.  2  (ACM,P1,P2,A1,A2,A12)
    0         .338       .082       -26.67   -26.67        .00
   45         .313       .225         5.10   -73.67      78.77
   90         .251       .402        41.77   -62.09     103.87
  135         .184       .528        89.77   -44.86     134.63
  180         .154       .574       153.33   -26.67     180.00
```

A. (Continued)

```
********************
 ACM   ALAB            PLAB            TLAB            BETA-GAMMA
 2.83301   .271475     49.6144         48.8602         65.2821
     -31.3327          .452071         7.99575E-02     .365162
          T(T T0 B)= -6.00003E-02
     DECAY 0F PARTICLE N0.  1  (ACM,P1,P2,A1,A2,A12)
    0       47.898      1.716        .27       .27        .00
   45       41.136      8.483        .62     -1.42       2.04
   90       24.810     24.810       1.09      -.55       1.63
  135        8.483     41.136       1.96      -.08       2.04
  180        1.716     47.898        .27       .27        .00
     DECAY 0F PARTICLE N0.  2  (ACM,P1,P2,A1,A2,A12)
    0         .347       .105     -31.33    -31.33        .00
   45         .320       .242       -.36    -74.23      73.88
   90         .253       .423      35.64    -64.78     100.42
  135         .182       .554      83.53    -48.66     132.19
  180         .149       .601     148.67    -31.33      180.00
********************
 ACM   ALAB            PLAB            TLAB            BETA-GAMMA
 3.30023   .316269     49.6038         48.8496         65.2681
     -34.5937          .482269         9.06185E-02     .389555
          T(T T0 B)= -8.00003E-02
     DECAY 0F PARTICLE N0.  1  (ACM,P1,P2,A1,A2,A12)
    0       47.888      1.716        .32       .32        .00
   45       41.127      8.481        .66     -1.37       2.04
   90       24.804     24.804       1.13      -.50       1.63
  135        8.481     41.127       2.01      -.03       2.04
  180        1.716     47.888        .32       .32        .00
     DECAY 0F PARTICLE N0.  2  (ACM,P1,P2,A1,A2,A12)
    0         .356       .126     -34.59    -34.59        .00
   45         .327       .259      -4.34    -74.15      69.81
   90         .256       .443      31.01    -66.36      97.37
  135         .180       .577      78.76    -51.18     129.94
  180         .144       .627     145.41     -34.59      180.00
********************
 ACM   ALAB            PLAB            TLAB            BETA-GAMMA
 3.70912   .355479     49.5931         48.8389         65.2541
     -37.0306          .510907         .101279         .412687
          T(T T0 B)= -.1
     DECAY 0F PARTICLE N0.  1  (ACM,P1,P2,A1,A2,A12)
    0       47.877      1.716        .36       .36        .00
   45       41.118      8.480        .70     -1.33       2.04
   90       24.799     24.799       1.17      -.46       1.63
  135        8.480     41.118       2.05       .01       2.04
  180        1.716     47.877        .36       .36        .00
     DECAY 0F PARTICLE N0.  2  (ACM,P1,P2,A1,A2,A12)
    0         .364       .147     -37.03    -37.03        .00
   45         .334       .275      -7.44    -73.81      66.37
   90         .259       .462      27.31    -67.34      94.65
  135         .178       .600      74.89    -52.97     127.86
  180         .140       .651     142.97     -37.03      180.00
```

A. (Continued)

```
********************
 ACM  ALAB            PLAB            TLAB            BETA-GAMMA
 7.53646  .723059     49.4332         48.679          65.0436
    -47.5423          .845541         .261195         .68299
          T(T T0 B)= -.400001
    DECAY 0F PARTICLE N0.  1  (ACM,P1,P2,A1,A2,A12)
  135        8.452     40.985          2.42            .37          2.05
  144        6.108     43.330          2.67            .45          2.23
  153        4.221     45.216          2.90            .52          2.38
  162        2.838     46.597          2.93            .59          2.34
  171        1.994     47.440          2.31            .66          1.66
  180        1.710     47.723           .72            .72           .00
    DECAY 0F PARTICLE N0.  2  (ACM,P1,P2,A1,A2,A12)
  135         .165       .875         47.40         -58.40        105.80
  144         .144       .899         59.89         -56.31        116.20
  153         .125       .918         74.47         -54.16        128.64
  162         .110       .931         91.54         -51.98        143.52
  171         .100       .940        111.14         -49.77        160.91
  180         .097       .943        132.46         -47.54        180.00
********************
 ACM  ALAB            PLAB            TLAB            BETA-GAMMA
 10.6927  1.02733     49.2199         48.4658         64.763
    -48.2372          1.1831          .474414         .955652
          T(T T0 B)= -.800002
    DECAY 0F PARTICLE N0.  1  (ACM,P1,P2,A1,A2,A12)
  135        8.416     40.809          2.73            .68          2.05
  144        6.081     43.143          2.99            .75          2.24
  153        4.203     45.021          3.22            .82          2.39
  162        2.826     46.396          3.24            .89          2.35
  171        1.986     47.235          2.62            .96          1.66
  180        1.703     47.517          1.03           1.03           .00
    DECAY 0F PARTICLE N0.  2  (ACM,P1,P2,A1,A2,A12)
  135         .168      1.163         30.99         -56.38         87.38
  144         .137      1.193         42.39         -54.84         97.23
  153         .109      1.216         56.55         -53.23        109.79
  162         .086      1.233         75.06         -51.59        126.64
  171         .069      1.243        100.09         -49.92        150.01
  180         .063      1.246        131.76         -48.24        180.00
********************
 ACM  ALAB            PLAB            TLAB            BETA-GAMMA
 13.1163  1.26199     49.0067         48.2526         64.4825
    -47.0361          1.47493         .687634         1.19138
          T(T T0 B)= -1.2
    DECAY 0F PARTICLE N0.  1  (ACM,P1,P2,A1,A2,A12)
  135        8.379     40.632          2.97            .91          2.06
  144        6.055     42.956          3.23            .98          2.24
  153        4.184     44.826          3.46           1.06          2.40
  162        2.814     46.195          3.49           1.13          2.36
  171        1.977     47.030          2.87           1.19          1.67
  180        1.695     47.311          1.26           1.26           .00
    DECAY 0F PARTICLE N0.  2  (ACM,P1,P2,A1,A2,A12)
  135         .178      1.418         20.86         -53.72         74.58
  144         .140      1.451         30.62         -52.45         83.07
  153         .106      1.478         42.82         -51.14         93.97
  162         .075      1.498         59.59         -49.79        109.39
  171         .050      1.510         86.62         -48.42        135.04
  180         .039      1.514        132.96         -47.04        180.00
```

B. $\pi + p \rightarrow \rho + \Delta$ 100 GeV/c

$\rho \rightarrow \pi + \pi$ $\Delta \rightarrow \pi + p$

```
********************
 ACM   ALAB            PLAB            TLAB            BETA-GAMMA
 0     0               99.6482         98.8911         131.116
       0               .351822         .049021         .284186
          T(T T0 B)= -1.96339E-03
     DECAY 0F PARTICLE N0.  1  (ACM,P1,P2,A1,A2,A12)
    0       96.197      3.452          .00      .00          .00
   45       82.615     17.036          .17     -.84         1.01
   90       49.825     49.825          .41     -.41          .81
  135       17.036     82.615          .84     -.17         1.01
  180        3.452     96.197          .00     -.00          .00
     DECAY 0F PARTICLE N0.  2  (ACM,P1,P2,A1,A2,A12)
    0         .320       .032          .00      .00          .00
   45         .298       .195        33.56   -57.94        91.50
   90         .246       .360        71.69   -40.33       112.02
  135         .190       .476       119.76   -20.28       140.04
  180         .165       .517       180.00     -.00       180.00
********************
 ACM   ALAB            PLAB            TLAB            BETA-GAMMA
 8.4131   .574075      99.1162         98.3591         130.416
    -48.1712          1.33274         .581025         1.07653
          T(T T0 B)= -1.
     DECAY 0F PARTICLE N0.  1  (ACM,P1,P2,A1,A2,A12)
    0       95.683      3.433          .57      .57          .00
   45       82.174     16.945          .75     -.27         1.02
   90       49.559     49.559          .98      .17          .82
  135       16.945     82.174         1.42      .40         1.02
  180        3.433     95.683          .57      .57          .00
     DECAY 0F PARTICLE N0.  2  (ACM,P1,P2,A1,A2,A12)
    0         .635       .698       -48.17   -48.17          .00
   45         .559       .815       -31.03   -59.84        28.81
   90         .374      1.066        -9.59   -60.80        51.22
  135         .172      1.293        24.97   -55.50        80.46
  180         .050      1.383       131.83   -48.17       180.00
********************
 ACM   ALAB            PLAB            TLAB            BETA-GAMMA
 11.9145  .814455      98.5831         97.826          129.715
    -44.4822          1.9999          1.11407         1.61543
          T(T T0 B)= -2.
     DECAY 0F PARTICLE N0.  1  (ACM,P1,P2,A1,A2,A12)
    0       95.168      3.415          .81      .81          .00
   45       81.732     16.854          .99     -.04         1.03
   90       49.293     49.293         1.23      .40          .82
  135       16.854     81.732         1.66      .64         1.03
  180        3.415     95.168          .81      .81          .00
     DECAY 0F PARTICLE N0.  2  (ACM,P1,P2,A1,A2,A12)
    0         .882      1.118       -44.48   -44.48          .00
   45         .770      1.259       -32.11   -52.01        19.90
   90         .497      1.579       -16.48   -52.98        36.49
  135         .207      1.882         8.29   -49.51        57.80
  180         .004      2.004       135.52   -44.48       180.00
```

C. $\pi + p \rightarrow \rho + \Delta$ 25 GeV/c

$\rho \rightarrow \pi + \pi$ $\Delta \rightarrow \pi + p$

```
********************
 ACM   ALAB            PLAB            TLAB            BETA-GAMMA
 0     0               24.6364         23.8881         32.4163
       0               .363633         5.22995E-02     .293726
          T(T T0 B)= -8.11387E-03
      DECAY 0F PARTICLE N0.  1  (ACM,P1,P2,A1,A2,A12)
    0       23.788       .848        .00      .00        .00
   45       20.430      4.215        .70    -3.40       4.10
   90       12.323     12.323       1.64    -1.64       3.29
  135        4.215     20.430       3.40     -.70       4.10
  180         .848     23.788        .00     -.00        .00
      DECAY 0F PARTICLE N0.  2  (ACM,P1,P2,A1,A2,A12)
    0         .323       .041        .00      .00        .00
   45         .301       .199      33.24   -55.80      89.04
   90         .246       .367      71.12   -39.40     110.52
  135         .189       .485     119.19   -19.89     139.08
  180         .163       .527     180.00     -.00     180.00
********************
 ACM   ALAB            PLAB            TLAB            BETA-GAMMA
 17.116   2.30992      24.1074         23.3594         31.7202
     -46.8072         1.33274         .581024         1.07653
          T(T T0 B)= -1.
      DECAY 0F PARTICLE N0.  1  (ACM,P1,P2,A1,A2,A12)
    0       23.278       .830       2.31     2.31        .00
   45       19.992      4.125       3.03    -1.17       4.19
   90       12.059     12.059       3.99      .63       3.36
  135        4.125     19.992       5.79     1.59       4.19
  180         .830     23.278       2.31     2.31        .00
      DECAY 0F PARTICLE N0.  2  (ACM,P1,P2,A1,A2,A12)
    0         .635       .698     -46.81   -46.81        .00
   45         .559       .815     -29.66   -58.48      28.81
   90         .374      1.066      -8.22   -59.44      51.22
  135         .172      1.293      26.33   -54.13      80.46
  180         .050      1.383     133.19   -46.81     180.00
********************
 ACM   ALAB            PLAB            TLAB            BETA-GAMMA
 24.3478  3.30996      23.5741         22.8263         31.0185
     -42.8896         1.9999          1.11407         1.61543
          T(T T0 B)= -2.
      DECAY 0F PARTICLE N0.  1  (ACM,P1,P2,A1,A2,A12)
    0       22.763       .811       3.31     3.31        .00
   45       19.550      4.034       4.04     -.24       4.29
   90       11.792     11.792       5.03     1.59       3.44
  135        4.034     19.550       6.86     2.58       4.29
  180         .811     22.763       3.31     3.31        .00
      DECAY 0F PARTICLE N0.  2  (ACM,P1,P2,A1,A2,A12)
    0         .882      1.118     -42.89   -42.89        .00
   45         .770      1.259     -30.52   -50.41      19.90
   90         .497      1.579     -14.89   -51.38      36.49
  135         .207      1.882       9.88   -47.92      57.80
  180         .004      2.004     137.11   -42.89     180.00
```

D. $K + p \rightarrow K^{*}(890) + \Delta(1238)$ 50 GeV/c

$K^{*}(890) \rightarrow K(494) + \pi(139)$; $\Delta(1238) \rightarrow \pi(139) + p(938)$

```
********************
 ACM   ALAB            PLAB            TLAB            BETA-GAMMA
 0     0               49.6444         48.7624         55.7802
       0               .355594         5.00571E-02     .287232
            T(T T0 B)= -3.90703E-03
      DECAY 0F PARTICLE N0.  1  (ACM,P1,P2,A1,A2,A12)
    0       47.867      1.777        .00       .00         .00
   45       43.181      6.467        .27     -1.80        2.07
   90       31.865     17.783        .52      -.92        1.44
  135       20.549     29.097        .57      -.40         .96
  180       15.861     33.784        .00      -.00         .00
      DECAY 0F PARTICLE N0.  2  (ACM,P1,P2,A1,A2,A12)
    0         .321       .035        .00       .00         .00
   45         .299       .196      33.46    -57.24       90.70
   90         .246       .363      71.51    -40.03      111.54
  135         .190       .478     119.58    -20.16      139.73
  180         .165       .520     180.00      -.00      180.00
********************
 ACM   ALAB            PLAB            TLAB            BETA-GAMMA
 11.9795  1.15047      49.1134         48.2314         55.1835
     -47.7235         1.33274         .581024         1.07653
            T(T T0 B)= -1.
      DECAY 0F PARTICLE N0.  1  (ACM,P1,P2,A1,A2,A12)
    0       47.355      1.758       1.15      1.15         .00
   45       42.719      6.398       1.42      -.67        2.09
   90       31.525     17.592       1.67       .22        1.46
  135       20.329     28.786       1.72       .75         .98
  180       15.691     33.422       1.15      1.15         .00
      DECAY 0F PARTICLE N0.  2  (ACM,P1,P2,A1,A2,A12)
    0         .635       .698     -47.72    -47.72         .00
   45         .559       .815     -30.58    -59.39       28.81
   90         .374      1.066      -9.14    -60.35       51.22
  135         .172      1.293      25.41    -55.05       80.46
  180         .050      1.383     132.28    -47.72      180.00
********************
 ACM   ALAB            PLAB            TLAB            BETA-GAMMA
 16.9895  1.63747      48.5802         47.6984         54.5845
     -43.9581         1.9999          1.11407         1.61543
            T(T T0 B)= -2.
      DECAY 0F PARTICLE N0.  1  (ACM,P1,P2,A1,A2,A12)
    0       46.841      1.739       1.64      1.64         .00
   45       42.255      6.329       1.91      -.20        2.11
   90       31.182     17.401       2.16       .69        1.47
  135       20.109     28.473       2.22      1.23         .99
  180       15.521     33.059       1.64      1.64         .00
      DECAY 0F PARTICLE N0.  2  (ACM,P1,P2,A1,A2,A12)
    0         .882      1.118     -43.96    -43.96         .00
   45         .770      1.259     -31.59    -51.48       19.90
   90         .497      1.579     -15.96    -52.45       36.49
  135         .207      1.882       8.81    -48.98       57.80
  180         .004      2.004     136.04    -43.96      180.00
```

REFERENCES

[1]M. LeBellac, Phys. Letters 25B, 524 (1967).

[2]M. Aderholz et al., Phys. Letters 27B, 174 (1968). (Aachen, Berlin, CERN collaboration.)

[3]J. T. Donohue, Nuovo Cimento LV, 527 (1968).

[4]M. Deutschmann et al., Phys. Letters 19, 608 (1965). (Aachen, Berlin, CERN collaboration.)

[5]K. Strauch, Remarks on Doing Strong-Interaction Physics Involving Multiparticle Final States in the 100-BeV Region, National Accelerator Laboratory 1968 Summer Study Report C.3-68-98, Vol. III, p. 281.

[6]D. I. Meyer, Spark-Chamber Experiment On $\pi^- + p \rightarrow N^* + \rho^0$, National Accelerator Laboratory 1968 Summer Study Report C.1-68-62, Vol. III, p. 93.

[7]Dr. George Kalbfleisch, A. Prodell, and associates have had some success with counters inside the liquid of the bubble chamber itself. Such procedures may be necessary.

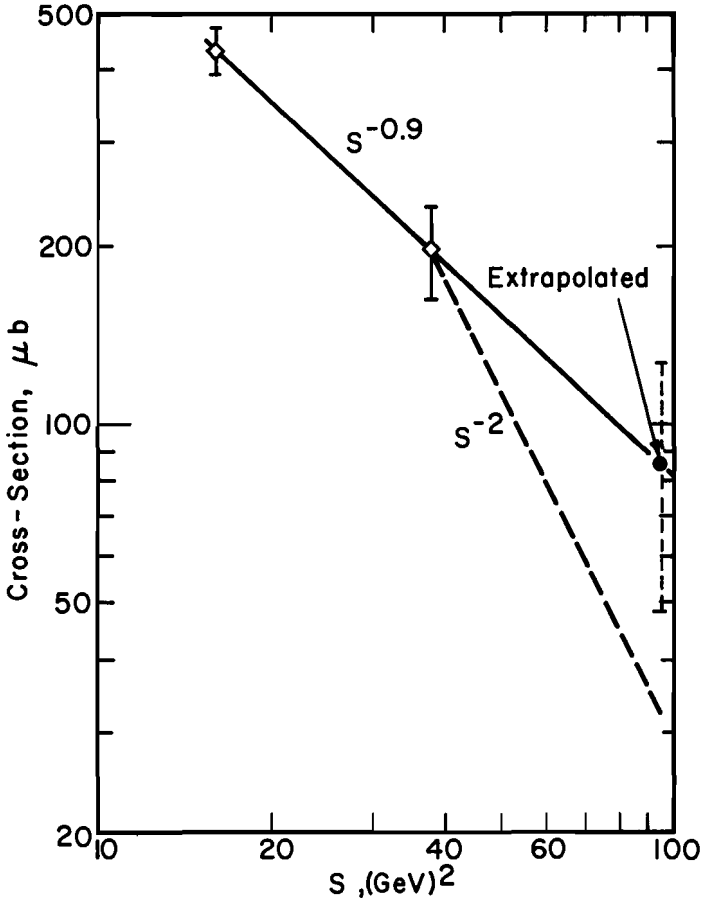

Fig. 1. Cross section for the reaction $\pi^+ p \rightarrow \rho^o \Delta^{++}$ as a function of S.

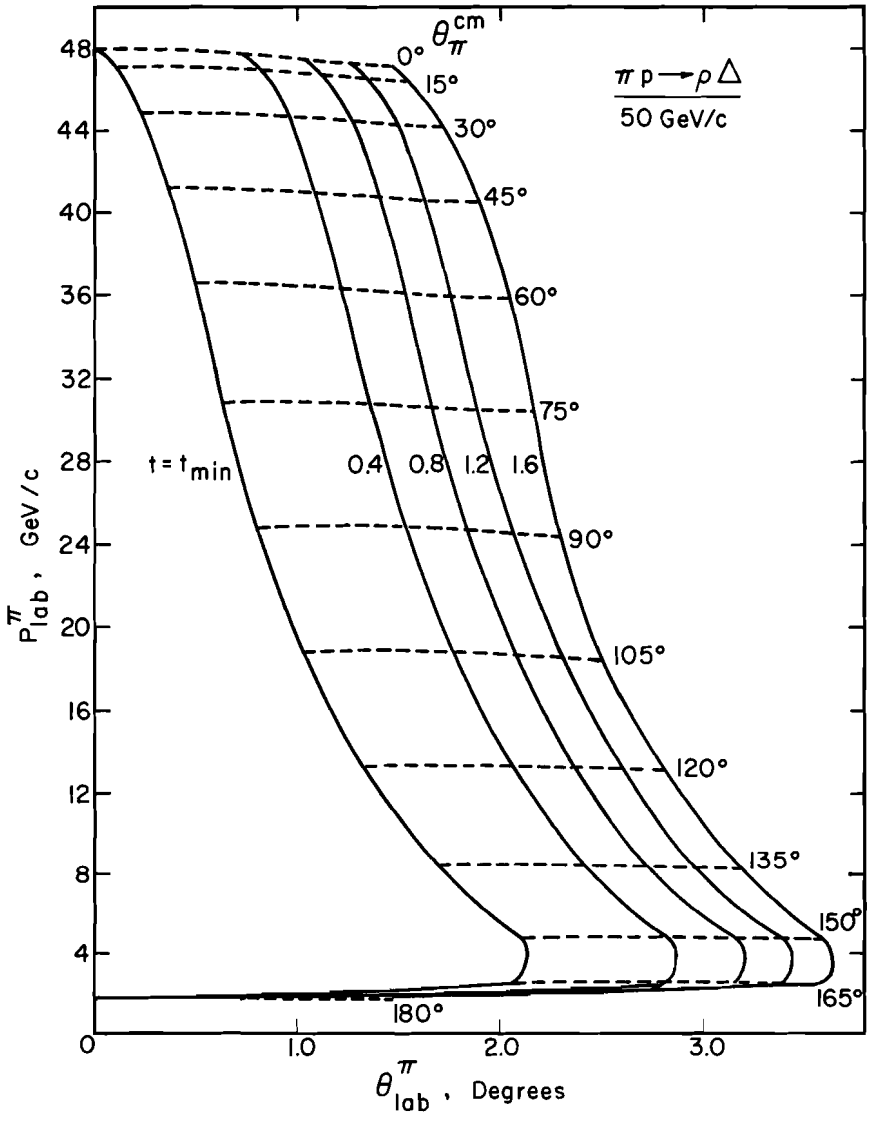

Fig. 2. Laboratory momentum vs laboratory angle for the pion from the rho decay in the process $\pi p \rightarrow \rho\Delta$ at 50 BeV/c. The angle shown is the largest angle from the incident beam direction.

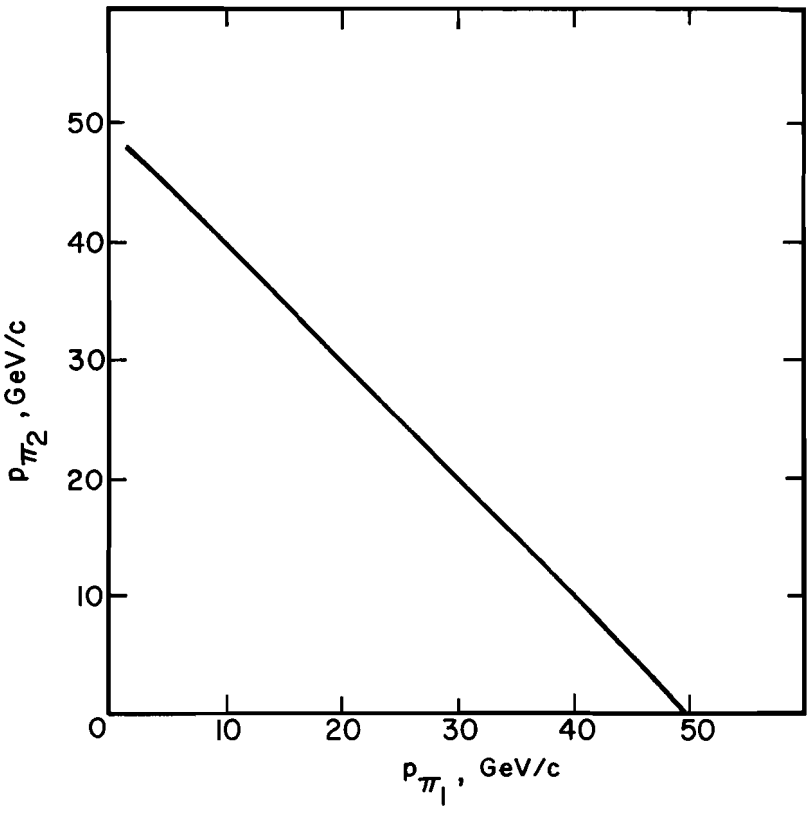

Fig. 3. Functional relation of the laboratory momenta of the pions from rho decay. Curve is essentially independent of t.

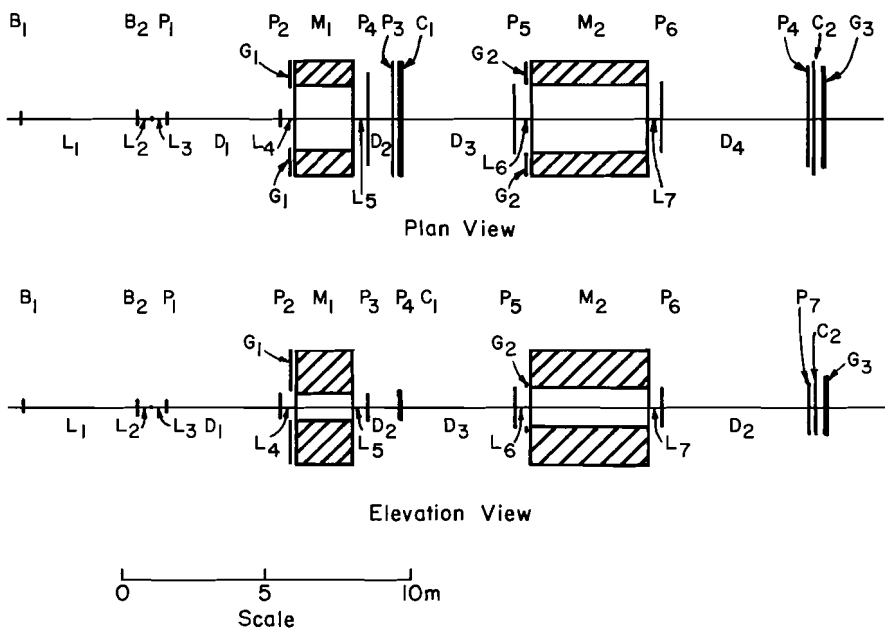

Fig. 4. Schematic view of the downstream spectrometer.

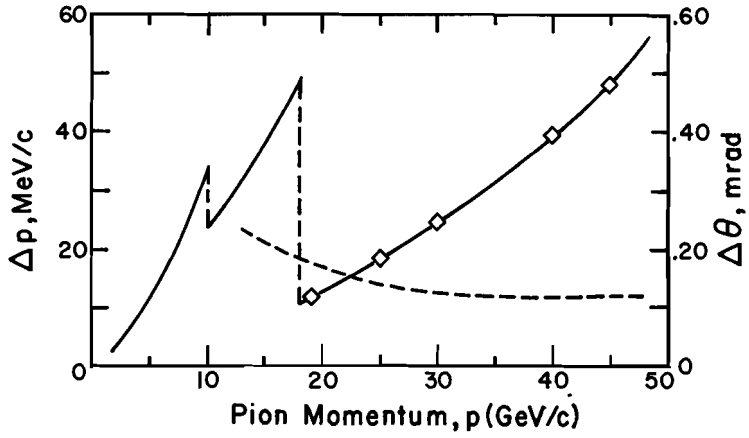

Fig. 5. Pion decay angles in the ρ produced at $t = t_{min}$. The curve is practically independent of t up to $t = -1.2$ $(GeV/c)^2$.

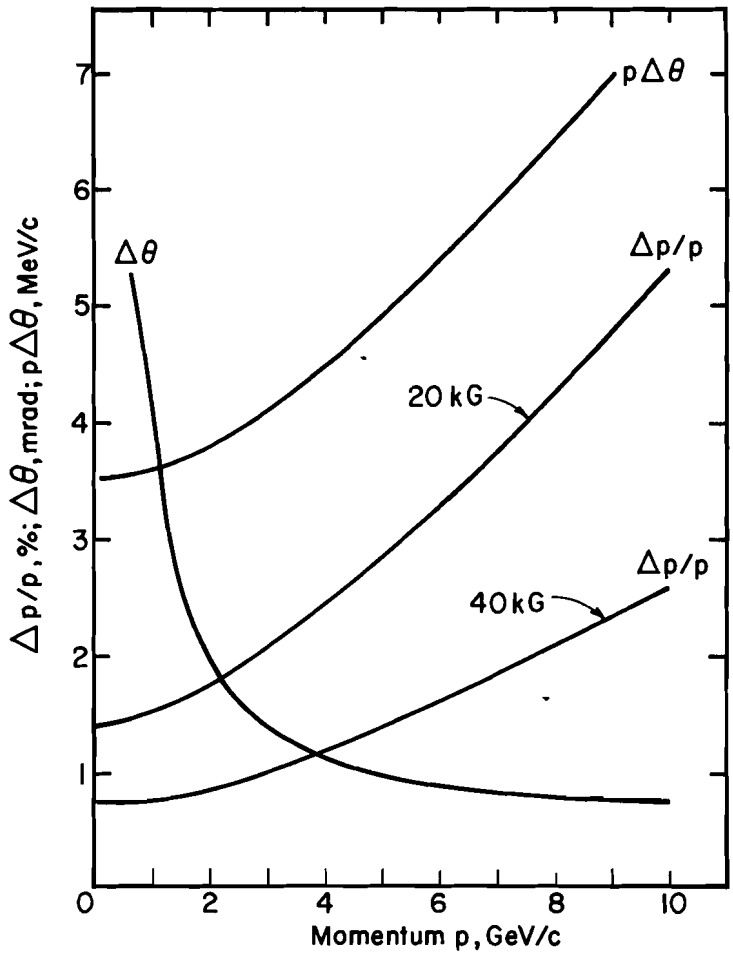

Fig. 6. Accuracy of momentum and angle measurement for a target bubble chamber.

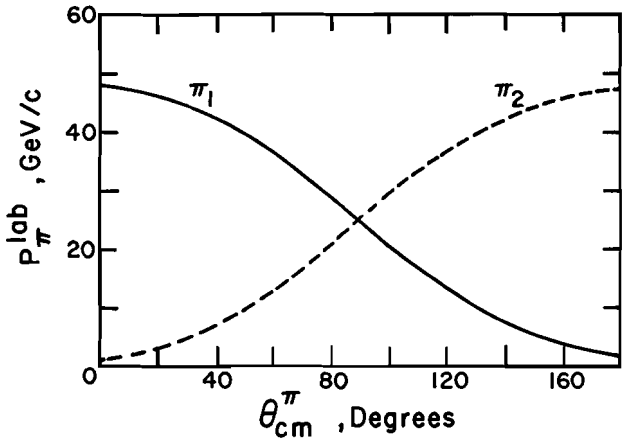

Fig. 7. Errors in momentum and angle of pions measured in the downstream spectrometer.

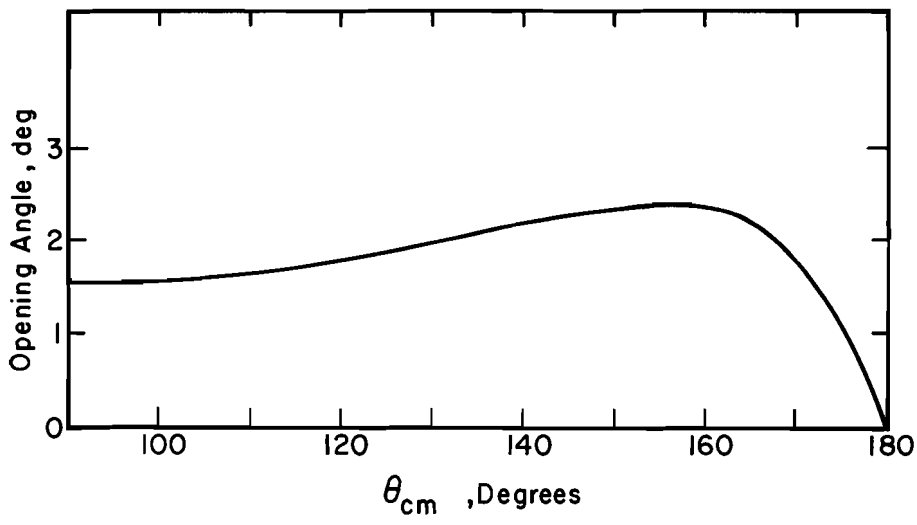

Fig. 8. Opening angle of the pions from ρ decay as a function of pion decay angle in the ρ center-of-mass, for a ρ produced at $t = t_{min}$ in the reaction $\pi p \rightarrow \rho\Delta$. Again, this curve is independent of t up to $t = -1.2\ (GeV/c)^2$.

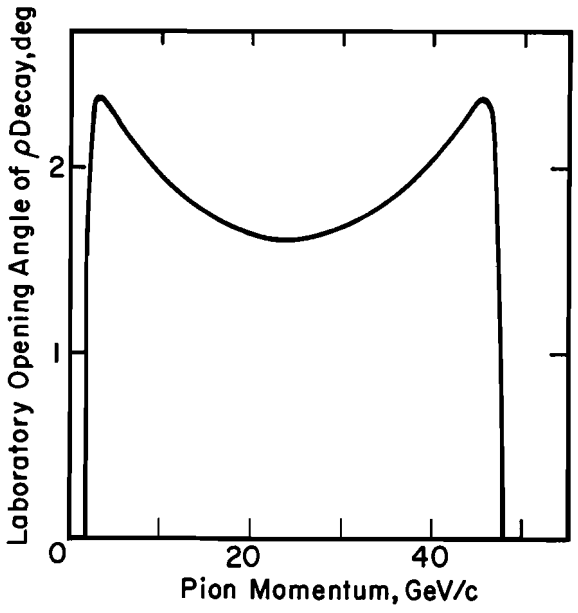

Fig. 9. Laboratory momentum of pion from ρ decay as a function of the laboratory opening angle of the ρ. [$t = t_{min}$, curve essentially independent of t up to $t = -1.2$ $(GeV/c)^2$.]

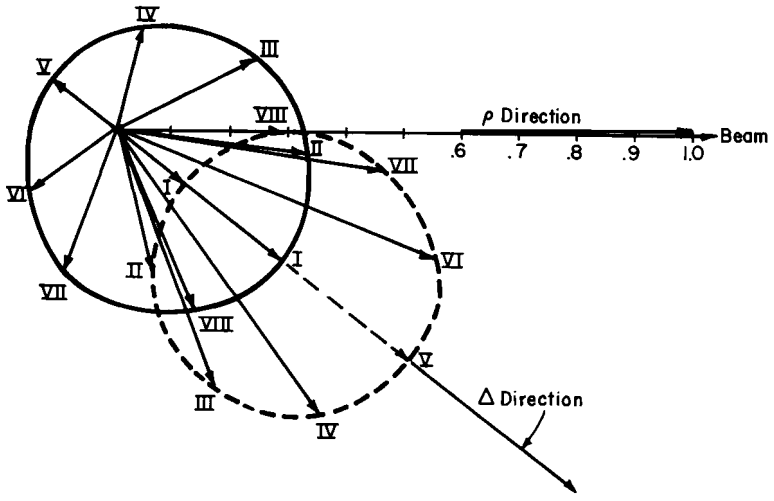

Fig. 10. Proton and pion momentum vectors resulting from the decay of the Δ in the reaction $\pi p \rightarrow \rho\Delta$ at an incident beam momentum of 50 BeV/c and different values of momentum transfer. The long forward arrow indicates the direction of the rho. Vector I is for a decay pion with a center-of-mass angle, in the Δ frame, of 0° relative to the Δ direction, II for 45°, III for 90°, etc. The dotted lines are pion vectors and the solid lines are the equivalent proton vectors. (a) $t_{p \rightarrow \Delta} = t_{min}$.

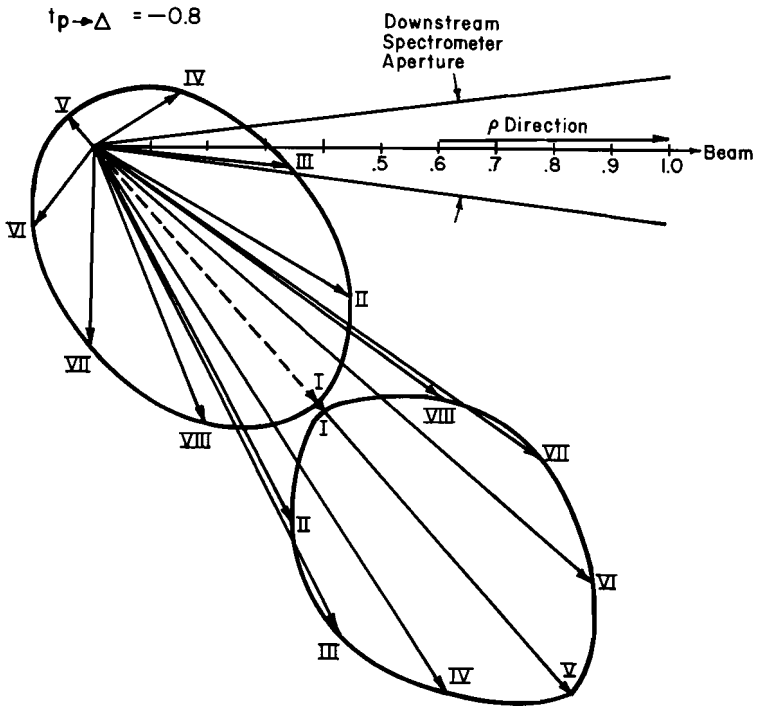

Fig. 10. Proton and pion momentum vectors resulting from the decay of the Δ in the reaction $\pi p \to \rho\Delta$ at an incident beam momentum of 50 BeV/c and different values of momentum transfer. The long forward arrow indicates the direction of the rho. Vector I is for a decay pion with a center-of-mass angle, in the Δ frame, of 0° relative to the Δ direction, II for 45°, III for 90°, etc. The dotted lines are pion vectors and the solid lines are the equivalent proton vectors. (b) $t_{p\to\Delta} = -0.8$.

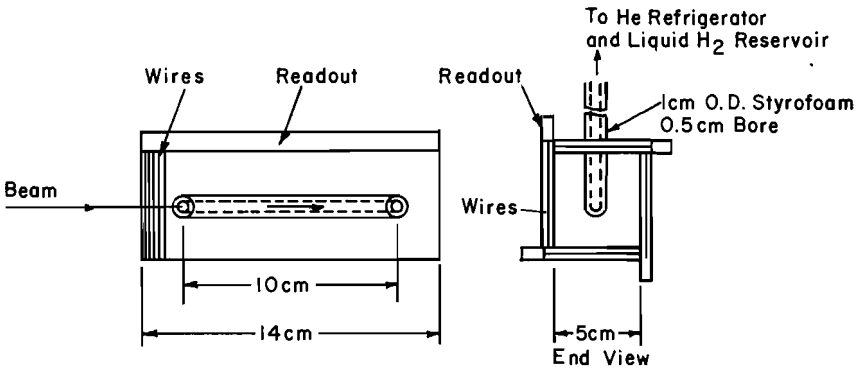

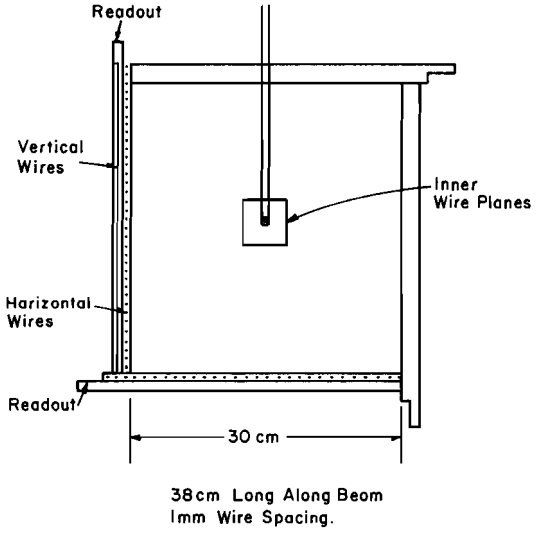

Fig. 11. Details of the target geometry showing the location of the wire planes and the target.

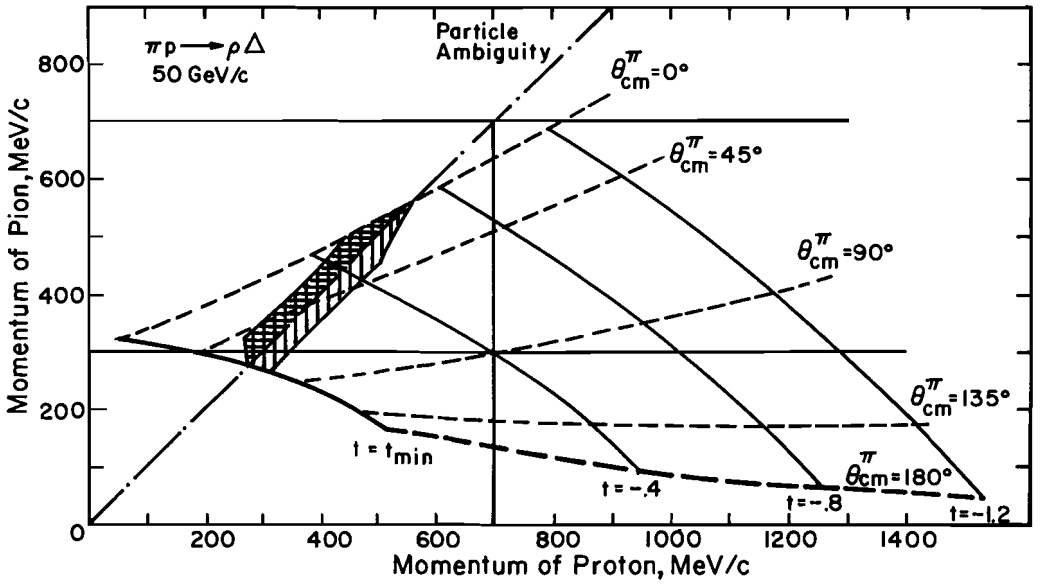

Fig. 12. Momentum of pion vs the momentum of the proton for decay of the Δ in the reaction πp → ρΔ. A particle identification problem exists when the momenta are nearly equal.